RSC Advances

ROYAL SOCIETY OF CHEMISTRY

www.rsc.org/advances

On the study of the relationship between thermal stability of Au catalysts and the basic nature of their supports for aerobic oxidation of benzyl alcohol

Chunli Xu [a,b,*], Zhen Wang [a,b], Xiuting Huangfu [a,b], Hanfei Wang [a,b]

[a] Key Laboratory of Applied Surface and Colloid Chemistry (Shaanxi Normal University), Ministry of Education, Xi'an 710119, PR China. E-mail: xuchunli@snnu.edu.cn

[b] School of Chemistry and Chemical Engineering, Shaanxi Normal University, 620 Chang'an West Street, Xi'an 710119, PR China

* Corresponding author. E-mail: xuchunli@snnu.edu.cn

Address for correspondence: School of Chemistry and Chemical Engineering
Shaanxi Normal University
620 Chang'an West Street
Xi'an 710119, P. R. China
Tel: 86-29-81530779
E-mail: xuchunli@snnu.edu.cn

Abstract

Gold catalysts were loaded on supports of hydrotalcite (HT), MgO, or γ-Al_2O_3 using methods of sol-immobilisation, deposition-precipitation or impregnation method. The aim of this work was to study the effect of basic property of supports on catalytic activity and thermal stability of gold catalyst in the benzyl alcohol oxidation reaction. Structure and property of supports and catalysts were characterized using techniques of X-ray diffraction patterns, scanning transmission electron microscopy, transmission electron microscopy, Hammett indicator, and N_2 physisorption. Gold particles prepared with sol-immobilisation method were the smallest, the most evenly dispersed, and had the best catalytic activity and lowest thermal stability. Nano-gold catalysts prepared with the other two methods had a lower catalytic activity and a good thermal stability. The thermal stability of gold catalyst varied with supports. The thermal stability of Au/HT and Au/MgO was better than that of Au/γ-Al_2O_3. It was found that the high thermal stability of Au/HT and Au/MgO was ascribed to basic property of their supports. The finding is instructive to design Au catalysts of high activity.

Keyword: molecular oxygen, oxidation, gold catalysts, solid base, thermal stability

1. Introduction

The selective oxidation of alcohols with molecular oxygen over

catalysts offers a sustainable, environmentally benign alternative to traditional processes that use expensive inorganic oxidants [1]. Recently, considerable attention has been devoted to the application of nano gold catalysts in the selective aerobic oxidation of alcohols [2]. Using a suitable support and a suitable preparation method, the gold catalysts are designed for high activity, selectivity, and mechanical strength [3, 4]. However, catalysts undergo deactivation, with poisoning, fouling, sintering, and volatilization being some of the common reasons for loss of catalyst activity [5]. For supported metal catalysts, sintering of metal particles is a major cause of catalyst deactivation [6]. The rate and extent of sintering of supported metals depend on support, promoter, and preparation method [5]. One of the driving forces of contemporary catalysis research is the rational design of novel catalytic materials [3-6]. The prerequisite of rational design are the identification of the influences of synthesis parameters on activity and thermal activity [7]. Based on the identification of property-determining parameters, a desired gold supported catalyst could be obtained by deliberate adjustment of the decisive synthesis parameters [7].

A key advantage in using gold, as compared to Pt and Pd, is the improved resistance of Au to overoxidation under liquid-phase oxidation conditions with O_2 as the oxidant [8]. However, in alcohol oxidation with gold catalysts, a severe limitation arises because of the necessary addition

of a homogeneous base to improve the oxidation kinetics and reduce deactivation [8]. The TOF associated with base-free conditions is generally an order of magnitude lower than the TOF obtained in high-pH conditions [9]. The addition of homogeneous base presents negative environmental and economic impacts since the high pH of the medium in corrosive and the salts of product need to be neutralized to release free acid [9]. As an alternative to adding homogeneous base, some groups investigated solid bases as catalyst supports, such as CeO_2 [10], TiO_2 [11], MgO [12], NiO [13], Al_2O_3 [14], Fe_2O_3 [11], and hydrotalcites (HT) [15]. However, to our knowledge, the effect of basic sites on the thermal stability of gold catalysts was not investigated.

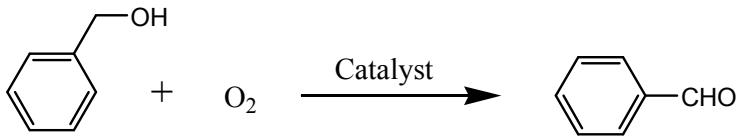

Scheme 1 Aerobic oxidation of benzyl alcohol

In this work, gold catalysts were loaded on supports of HT, MgO or γ-Al_2O_3 using methods of sol-immobilisation method (SI), deposition-precipitation (DP), or impregnation method (IMP). The benzyl alcohol oxidation is an important model reaction to test for oxidative activity and selectivity over supported metals [9]. The aim of this work was to study the effect of basic property of supports on catalytic activity and thermal stability of gold catalyst in the benzyl alcohol oxidation

reaction (Scheme 1).

2. Experimental

2.1 Preparation of catalysts

2.1.1 Preparation of supports

Preparation of HT

HT with Mg^{2+}/Al^{3+} atomic ratios of 5:1 were prepared using a co-precipitation method as described in our previous report [16]. An aqueous solution (166 mL) of the metal nitrates in the desired Mg^{2+}/Al^{3+} molar ratio, with a total concentration of 1.5 M, was mixed slowly with an alkaline solution of Na_2CO_3/NaOH with continuous stirring. The molar quantity of Na_2CO_3 employed was twice that of Al^{3+}. The pH value of the mixture was kept constant, typically at values between 9 and 10, by adjusting the rate of addition of the alkaline solution. The temperature was maintained at 25 °C, which resulted in the formation of heavy slurry, and the mixture was aged at 60 °C for 18 h with stirring, to enhance the selective formation of the precipitated HT phase. The slurry was then cooled to 25 °C, filtered, and washed with water until the pH value of the filtrate was near 7. The precipitate was dried at 90 °C for 16 h. The resulting materials were HT.

Preparation of mixed oxides and single oxide

The HT as-prepared, was calcined at 500 °C for 3 h in static air to generate Mg(Al)O.

MgO support was prepared by the thermal decomposition of $Mg(OH)_2$ using the same decomposition procedure as Mg(Al)O samples. The $Mg(OH)_2$ used was a commercial sample

The γ-Al_2O_3 used was a commercial sample (Alfa Aesar, S_{BET}=188 $m^2 g^{-1}$). It was activated at 500 °C for 3 h in static air before the reaction test.

2.1.2 Preparation of nano-Au-loaded catalyst

SI method

Au catalysts supported on different supports were prepared using a SI method described in literature [17]. Aqueous solutions of $HAuCl_4.4H_2O$ of the desired concentration were prepared. To this solution polyvinyl alcohol (PVA) was added such that the PVA to Au ratio was 1.2 by mass. Subsequently, a freshly prepared 0.1 M solution of $NaBH_4$ (> 96% purity, $NaBH_4$/Metal mole fraction = 4, Aldrich) was added to form a dark-brown sol. After 30 min of sol generation, the colloid was immobilized by adding supports under vigorous stirring. The amount of support material required was calculated to give a final metal loading of 1% by mass. After 2 h, the slurry was filtered, the catalyst washed thoroughly with distilled water and dried at 100 °C overnight.

DP method

The deposition–precipitation procedure was similar to method described in literature [18]. The obtained supports (1.0 g) was added to 30

mL of an aqueous solution of $HAuCl_4$ (Theoretical Au loading is 1 wt%). After stirring for 5 min, 0.2 mL of aqueous NaOH (0.5 M) was added and the resulting mixture was stirred at room temperature for 12 h. The obtained slurry was filtered, washed with deionized water, and dried at room temperature for 12 h. The solid was subsequently treated with aqueous $NaBH_4$ ($NaBH_4$/Metal mole fraction = 4) solution at room temperature for 2 h, then filtered, washed and dried to yield the Au catalyst.

IMP method

The catalyst was prepared by the wet impregnation method technique by contacting the support (1.0 g) with 30 mL of an aqueous acidic solution of $HAuCl_4.4H_2O$ containing the required amount of gold (Theoretical Au loading is 1 wt%), evaporating the water at 100 °C with vigorous stirring and drying in drying oven at 100 °C for 12 h and finally treated with aqueous $NaBH_4$ ($NaBH_4$/Metal mole fraction = 5) solution at room temperature for 2 h, then filtered, washed and dried to yield the Au catalyst.

Through the methods above, three types of catalysts, i.e. Au/HT, Au/MgO and Au/γ-Al_2O_3, were prepared. In order to study the thermal stability of catalysts prepared by various methods and supports, the obtained Au catalysts were calcined at 500 °C for 2 h in static air to produce the calcined samples.

2.2 Catalyst characterization

X-Ray diffraction patterns were recorded using a D/Max-3CX-raypowder diffractometer (Rigaku Co., Japan), using a Cu-Ka source fitted with an Inel CPS 120 hemisphericaldetector.

The surface area and pore characteristics of the catalysts were determined using a Micromeritics ASAP 2020 instrument. The sample was degassed at 250 °C for 4 h in N_2 prior to surface area measurement. Nitrogen adsorption and desorption isotherms were measured at -196 °C, and the specific surface areas of the catalysts were determined byapplying the BET (Brunauer-Emmett-Teller) method to nitrogena dsorption data obtained in the relative pressure range from 0.06 to 0.30. Total pore volumes were estimated from thea mount of nitrogen adsorbed at a relative pressure of 0.995. Pore volume and pore-size distribution curves were obtained from analysis of the desorption branches of the nitrogen isotherms using the BJH (Barrett-Joyner-Halenda) method.

Hammett indicator experiments were conducted to determine the basic strength of each catalyst. The Hammett indicators used were methyl yellow (pK_a = 3.3), methyl yellow (pK_a = 4.8), neutral red (pK_a = 6.8), bromothymolblue (pK_a = 7.2), phenolphthalein (pK_a = 9.3), alizarinyellowR (pK_a = 11.0), indigo carmine (pK_a = 12.2), 2,4-dinitroaniline (pK_a = 15), 4-nitroaniline (pK_a = 18.4), 4-chloroaniline (pK_a = 26.5), and diphenylmethane (pK_a = 35). Typically, 25mg of the

catalyst was mixed with 5mL of a solution of Hammett indicators diluted with cyclohexane and allowed to sit for at least 1 h. After the equilibration, the color of the catalyst was noted. The basic strength of the catalyst was taken to be higher than the weakest indicator that underwent a color change and lower than the strongest indicator that underwent no color change. To measure the basicity of solid bases, the method of Hammett indicator–benzene carboxylic acid (0.02 mol/L anhydrous ethanol solution) titration was used.

The gold loading of the catalysts was determined by Flame atomic absorption spectrometry. A TAS986 atomic absorption spectrophotometer was used, the wavelength range detected was 190 ~ 900 nm.

The Transmission Electron Microscopy (TEM) micrographs were obtained by using a JEM2010 instrument. The Scanning Transmission Electron Microscopy (STEM) micrographs were obtained by using a FEI Tecnal G2 F20 instrument.

2.3 Reaction procedure

The aerobic oxidation of benzyl alcohol was carried out in a two-necked round bottom flask equipped with a water-cooled condenser at 100 °C under vigorous stirring. Typically, the flask was charged with 0.25 g of catalyst, 1 mmol benzyl alcohol, and 10 mL toluene. The flask was then flushed with pure oxygen (Flow rate = 25 mL/min) and heated to 100 °C for 1 h. After the reaction, the catalyst was separated by

filtration. The reaction products were analyzed by gas chromatography (Shimadzu GC-2014) equipped with a flame ionization (FID) detector and an Rtx-wax column (30 m × 0.32 mm × 0.5 μm). Dodecane was used as an internal standard. For the determination of TOF, 0.05 g catalysts were used for 30 min of reaction time. Other reaction conditions were same with those of the typical reaction condition above.

3. Results and discussion

3.1 Catalyst characterization

3.1.1 BET surface area and pore size

As shown in Table 1, the BET surface areas of $Mg(OH)_2$, MgO, and the rehydrated $Mg(OH)_2$ were 19 $m^2 g^{-1}$, 174 $m^2 g^{-1}$, and 53 $m^2 g^{-1}$, respectively. This indicated that the surface area of MgO was far higher than that of its $Mg(OH)_2$ precursor. However, when MgO was rehydrated to form $Mg(OH)_2$, its surface area decreased greatly. The surface area of HT was 16 $m^2 g^{-1}$, while the surface area of Mg(Al)O was 145 $m^2 g^{-1}$. This indicated that surface area of Mg(Al)O was far higher than that of its precursor HT. The surface area of γ-Al_2O_3 was 188 $m^2 g^{-1}$, which was the largest among the investigated supports.

3.1.2 XRD analysis

Fig. 1 displays the XRD patterns of catalysts before and after calcination. The X-ray diffractograms of Au/γ-Al_2O_3 before and after calcination were similar, showing the typical X-ray diffractograms of

γ-Al_2O_3 (Fig. 1a) [16]. The X-ray diffractograms of Au/HT showed the typical X-ray diffractograms of HT, with characteristic diffraction peaks at 11.4°, 23.0° and 34.9° (Fig. 1b) [16]. The thermal pre-treatment resulted in a change in the XRD pattern, caused by the removal of CO_2 and H_2O from the starting material. The Au/HT after calcination displayed diffraction reflections characteristic of MgO [19, 20]. This indicated that the crystalline structure of Au/HT sample changed before and after calcination. The XRD patterns of Au/MgO before and after calcination are presented in Fig. 1d and 1e. It can be seen that the major phase present for the Au/MgO before calcination was $Mg(OH)_2$, while MgO was the major phase for Au /MgO after calcination [19, 20]. This demonstrated that MgO was rehydrated to form $Mg(OH)_2$, during the process of doping. After calcination, $Mg(OH)_2$ removed water to form MgO. No diffractograms of Au were observed for the supported catalysts, due to the low loading amount.

3.1.3 Gold size of catalysts

Fig. 2 displays the TEM images of the Au particles on different supports with different preparation methods. The size of Au on γ-Al_2O_3 was irrespective of the preparation methods (Fig. $2c_1$-c_3), while Au particles on HT (Fig. $2a_1$-a_3) or MgO (Fig. $2b_1$-b_3) were dependent on the preparation methods. All the samples of Au/γ-Al_2O_3 appeared to be uniformly coated with Au particles and had the lowest size of Au particles.

The mean size of gold particles on Au/γ-Al_2O_3 was around 3.4 nm (Table 2). For Au/HT and Au/MgO, only those prepared by SI methods (Fig. $2a_1$ and b_1) had as low size of Au particles as those of Au/γ-Al_2O_3. Those prepared by IMP method and DP method, showed larger size of Au particles (5.2 ~ 8.4 nm).

TEM images of catalysts after calcination were also measured. After clacination, Au particles by SI method coagulated apparently, those by the other two methods increased slightly in size. In order to further understand the change of gold particles before and after calcination, the STEM of samples were studied. Fig. 3 shows the STEM images and gold size distribution of Au/HT by IMP method before and after calcination. The mean size of gold particles was 6.4 nm before calcination, but it increased to 11.4 nm after calcination.

3.1.4 The basic property of the catalysts

The property of basic site is related to the state of O ions on the surface of supports [21]. In order to understand the state of O ions, the XPS spectra of O 1s for catalysts were determined (Fig. 4). On the surface of Au/MgO before calcination, "OH^-" surface content to the total amount of surface oxygen atoms was 63%, which was obtained by calculating the area of corresponding XPS peaks ($A_{OH^-} / A_{OH^-} + A_{O^-} + A_{O^{2-}} = 0.63$). This indicated that OH^- was the main basic sites on Au/MgO before calcination. For Au/MgO after calcination, "O^{2-}"

surface content to the total amount of surface oxygen atoms was 60%, suggesting that the main basic sites on Au/MgO after calcination catalyst was "O^{2-}". The results were in agreement with those by XRD analysis.

The strength of the basic sites in the supports was analyzed qualitatively using Hammett indicators. As shown in Table 3, γ-Al_2O_3 possessed H_- values in the range $7.2< H_-<9.3$ (Entry 6). $Mg(OH)_2$ (Entry 3), rehydrated $Mg(OH)_2$ (Entry 5), and HT (Entry 1) possessed H_- values in the range $9.3< H_-<11$ (Entry 2 and 3). H_- values of MgO (Entry 4) and Mg(Al)O (Entry 3) were in the range $12.2< H_-<15$. This means that MgO and Mg(Al)O had the strongest basic sites, next were $Mg(OH)_2$, rehydrated $Mg(OH)_2$, and HT, and γ-Al_2O_3 had the most weak basic sites.

The basicity of solid bases was also measured (Table 3). The total basicity of Mg(Al)O was 0.57 mmol/g (Entry 2), which was higher than that of its precursor HT (0.30 mmol/g, Entry 1). Similarly, the total basicity of MgO was 0.98 mmol/g (Entry 4), which was also higher than that of its precursor $Mg(OH)_2$ (0.36 mmol/g, Entry 3). The basicity of rehydrated $Mg(OH)_2$ was 0.42 mmol/g, which was higher than that of $Mg(OH)_2$, but lower than that of MgO. γ-Al_2O_3 (0.11 mmol/g) showed the lowest basicity (Entry 6). Therefore, both the basic strengths and basicity of MgO or Mg(Al)O were higher than those of their corresponding precursor $Mg(OH)_2$ or HT.

XRD analysis showed that the crystal phase of Au/HT before and

after calcination changed from HT before calcination to Mg(Al)O after calcination. The strength and number of basic sites on HT were lower than that of Mg(Al)O. Combining basic property of supports with XRD analysis, it was found that the strength and number of basic sites on Au/HT before calcination were lower than it after calcination. Similarly, the crystal phase of Au/MgO before calcination was $Mg(OH)_2$, while it changed to MgO after calcination. The strength and number of basic sites on $Mg(OH)_2$ were also lower than that of MgO. So the strength and number of basic sites on Au/MgO before calcination were also lower than it after calcination. In contrast, the XRD analysis showed that the crystal phase of Au/γ-Al_2O_3 before and after calcination did not change. Accordingly, the basic property of Au/γ-Al_2O_3 did not change before and after calcination.

3.1.5 Valence states of gold

We used XPS to characterize the valence states of gold. As shown in Fig. 5, Au/MgO before calcination contained only metallic Au^0 showing $4f_{7/2}$ and $4f_{5/2}$ signals at 83.7 and 87.6 eV, respectively [22]. Similar to Au/MgO before calcination, Au/MgO after calcination also contained only Au^0.

3.2 Effect of supports and preparation method on the activity of Au catalysts

Catalytic performance of catalysts was shown in Table 2. In terms of

preparation method, catalysts by SI method showed the highest catalytic activity for a certain support, whereas those by DP or IMP methods showed lower catalytic activity. Take the support of HT as one example. TOF of Au/HT by SI was 670 h^{-1} (Table 2, Entry 1), while TOF of Au/HT by DP or IMP was 459 (Table 2, Entry 4) and 280 h^{-1} (Table 2, Entry 7), respectively. The high activity of Au by SI method may be related to its size. The Au particles by SI method distributed uniformly and had the lowest size, which resulted in its high activity (Fig. 2). The Au particles by other two methods had higher size, explaining their lower activity.

In terms of supports, the catalytic activity of nano Au supported by HT or MgO was strongly dependent on the preparation methods. Take the support of MgO as one example. TOF of Au/MgO by SI method was as high as 494 h^{-1} (Table 2, entry 2), while those by DP or IMP method were 230 and 295 h^{-1} (Table 2, entries 5 and 8), respectively. In contrast to HT or MgO, preparation method showed lower effect on the activity of Au/γ-Al_2O_3. The TOF of Au/γ-Al_2O_3 was 552, 489 and 441 h^{-1} for SI method (Table 2, entry 3), DP (Table 2, entry 6) and IMP method (Table 2, entry 9), respectively. The effect of supports on activity of nano gold was ascribed to the effect of supports on size of nano gold. The size and distribution of Au particles on HT or MgO was strongly affected by the preparation method, while preparation methods showed low effect on the

size and distribution of Au particles on γ-Al_2O_3 (Fig. 2).

For a certain preparation method, the catalytic activity of nano Au varied with its support. In the case of Au prepared by SI method, Au/HT showed the highest activity (Table 2, entries 1 to 3). Each nano Au catalyst prepared by SI method had low size of particles, so the highest activity of Au/HT could be ascribed to its low size. The difference in the activity of Au by SI method may be due to the difference in the acid/base property of supports [15]. γ-Al_2O_3 and HT possessed both acid and basic sites, while $Mg(OH)_2$ and MgO only contained basic sites [15]. The basic strength of HT was higher than that of γ-Al_2O_3. The acid and basic sites of HT promoted the high activity of Au/HT by SI method. In contrast, Au/γ-Al_2O_3 showed the highest activity for Au prepared by DP (Table 2, entries 4 to 6) or IMP (Table 2, entries 7 to 9). For IMP method (Table 2, entries 7 to 9), the TOF of Au/γ-Al_2O_3 was 441 h^{-1}, which was higher than that of Au/MgO (295 h^{-1}) or Au/HT (280 h^{-1}). The high activity of Au/γ-Al_2O_3 was due to its low size of Au particles.

3.3 Effect of basic property and preparation method on thermal stability of catalysts

In order to test the thermal stability of catalysts, Au catalysts were calcined and determined in the aerobic oxidation of alcohol. As shown in Table 2, compared with catalyst before calcination, the activity of catalyst by SI method decreased apparently after calcination (Entries 1-3). Take

Au/HT by SI method as one example (Table 2, entry 1). The TOF of Au/HT by SI was 670 h^{-1} before calcination, and decreased to 240 h^{-1} after calcination. Similar phenomenon was observed for Au/MgO and Au/γ-Al_2O_3 by SI method. The deactivation of Au catalyst by SI method was consistent with the coagulation of Au particles after calcination (Fig. $2a_{1\text{-}cn}$, $b_{1\text{-}cn}$ and $c_{1\text{-}cn}$).

In contrast, the activity of Au catalyst by the other two methods did not decrease after calcination. It was found that the variation of catalyst before calcination versus catalyst after calcination depended on the property of supports (Table 2, entries 4-9). The activity of Au/HT and Au/MgO increased apparently after calcination. Take Au/MgO by DP method as one example (Table 2, entry 7). The TOF of Au/MgO before calcination was 230 h^{-1}, and it increased to 314 h^{-1} after calcination. The activity of Au/γ-Al_2O_3 did not change apparently after calcination. The TOF of Au/γ-Al_2O_3 before calcination was 489 h^{-1} and 441 h^{-1} for DP and IMP method, respectively. After calcination, it was 478 h^{-1} and 458 h^{-1} for DP and IMP method, respectively. The Au catalysts before and after calcination differed in three aspects, i.e. size of gold [23], valence of gold [22] and basic property of support [9,15]. Each of them could affect the activity of gold.

One argument showed the size of gold could not result in the increased activity of Au catalysts after calcination. Generally, the size of

gold is inversely proportional to its activity [23,24]. The higher the size of gold, the lower its activity is. Since the size of gold on Au/MgO and Au/HT after calcination was greater than that before calcination, the increased size of gold on Au/MgO and Au/HT would not facilitate the reaction rate, on the contrary, would reduce their activity. So, the higher activity of Au/MgO and Au/HT after calcination could not be ascribed to the effect of gold size.

Next consider the factor of oxidation state of gold. Due to importance of gold as heterogeneous catalysts, a significant degree of attention has been focused upon the elucidation of the active phase. Abad *et al.* tested active sites of Au/CeO_2 in oxidation of alcohol [22]. More recently, Zhao *et al.* also investigated the active sites of Au/Ni_2O_3 in oxidation of alcohol [25]. Both of them showed a direct correlation between the concentration of Au^+ or Au^0 species and catalyst supports. In this study, XPS spectrum demonstrated the presence of only Au^0 species. So the higher activity of Au/MgO and Au/HT after calcination could not be ascribed to the effect of valence state of gold.

Finally consider the factor of basic property of supports. The strength and amount of basic sites on Au/HT and Au/MgO after calcination was higher than that before calcination. Catalytic activity of gold is promoted by basic property of supports [9]. Since the two factors of size and valence state of gold had been ruled out, the increased activity

of Au/HT and Au/MgO after calcination should be ascribed to the change of their basic property after calcination. This proposal could be also applied to Au/γ-Al_2O_3. Since the basic property, valence state of gold, and size of gold on Au/γ-Al_2O_3 before and after calcination did not change apparently, its activity before calcination and after calcination should be also similar. The results in Table 2 did show that the activity of Au/γ-Al_2O_3 before calcination was similar to it after calcination. The consistency between the prediction and the experimental results further supported the proposal.

Since the activity of Au/HT and Au/MgO after calcination was higher than them before calcination, HT after calcination and MgO were better supports than HT before calcination and $Mg(OH)_2$, respectively. The results also gave one hint as below. The number of basic sites of MgO was far higher than that of its precursor $Mg(OH)_2$, which resulted in the higher activity of Au/MgO. In the traditional method of preparing gold catalyst, MgO transformed to $Mg(OH)_2$ because of the aqueous system. The hydrolysis of the MgO in aqueous solution of gold resulted in the decrease of number of basic sites. In order to increase the number of basic sites, Au/MgO was prepared by thermal decomposition of Au/$Mg(OH)_2$. During the process of calcination, although the number of basic sites was increased, the size of gold was also raised up because of the sintering of gold particles in the high temperature. The number of

basic sites was proportional to the activity of gold, while the size of gold was reverse. If one method was designed to make the number of basic sites of MgO and size of gold unchanged during the process of preparing the Au/MgO catalyst, the obtained Au/MgO should show high activity. Enlightened by this, we are trying to design a new method of preparing Au/MgO. In this new method, the Au/MgO would keep both basic sites of MgO and low size of gold nanoparticles.

3.4 Reusibility of catalysts

The reusability of catalyst was important for application of catalysts in industry. Table 4 displays the results of recycling experiments of catalysts by SI method. The conversions of fresh catalysts were in the range of 95-100%. In the second use, the conversion of Au/HT was 97%, which was similar with that of the fresh one. The conversion of Au/MgO and Au/γ-Al_2O_3 decreased apparently in the second run. The conversion of Au/γ-Al_2O_3 decreased from 97% in the first run to 57% in the second run. The decreased conversion of Au/MgO was more than that of Au/γ-Al_2O_3 in the second run. The conversion of Au/MgO decreased from 95% in the first run to 31% in the second run. In the third run, the conversion of Au/HT was 85%, while the conversion of Au/γ-Al_2O_3 was only 38%. The conversion of Au/MgO in the third run was not determined since its low activity in the second run. The results indicated that Au/HT had the highest reusability, next was Au/γ-Al_2O_3, and

Au/MgO had the lowest reusibility.

The difference in the reusibility of catalysts may be due to the stability of gold particles. The difference in size of gold particles between catalysts before reaction and after two run was determined (Table 4). Compared with the fresh catalysts, the size of gold particles on all the spent catalysts increased. After two run, the size of gold particles on Au/HT increased 0.1 nm, while it increased 0.5 nm for Au/γ-Al_2O_3 catalysts. Part of gold particles on Au/MgO coagulated. This indicated that Au/HT had the highest stability, next was Au/γ-Al_2O_3, and Au/MgO had the lowest stability. The stability of gold particles was in accordance with the reusability.

4. Conclusion

Thermal stability of gold particles was related to its preparation method, as well as structure and basic property of its support. Gold catalyst by SI method showed the lowest thermal stability. The thermal stability of Au catalyst by the other two methods (IMP and DP) varied with support types. The thermal stability of Au/HT and Au/MgO was better than that of Au/γ-Al_2O_3. It was found that the property and number of basic sites affected the thermal stability of gold. After calcination, Au/MgO and Au/HT changed not only in the property of basic sites, but also in the number of basic sites. The change in property and number of basic sites increased the thermal stability of Au/MgO and Au/HT. It was

also found that HT after calcination and MgO were better supports than HT before calcination and $Mg(OH)_2$, respectively. This work would be instructive for designing Au catalysts with high activity and thermal stability.

Acknowledgements

This work was supported by the National Natural Science Foundation of China (Program No. 21343015), Natural Science Basic Research Plan in Shaanxi Province of China (Program No. 2013JM2003), and the Fundamental Research Funds for the Central Universities (Program No. GK201302016).

References

[1] B.N. Zope, D.D. Hibbitts, M. Neurock and R.J. Davis, *Science*, 2010, **330**, 74–78.

[2] C.D. Pina, E. Falletta and M. Rossi, *Chem. Soc. Rev.*, 2012, **41**, 350–369.

[3] S. Wang, Q. Zhao, H. Wei, J. Wang, M. Cho, H.S. Cho, O. Terasaki and Y. Wan, *J. Am. Chem. Soc.*, 2013, **135**, 11849−11860.

[4] G.M. Veith, A.R. Lupini, S. Rashkeev, S.J. Pennycook, D.R. Mullins, V. Schwartz, C.A. Bridges and N.J. Dudney, **J. Catal.**, 2009, **262**, 92–101.

[5] M.T. Bore, H.N. Pham, E.E. Switzer, T.L. Ward, A. Fukuoka and A.K. Datye, *J. Phys. Chem. B*, 2005, **109**, 2873–2880.

[6] X. Yan, X. Wang, Y. Tang, G. Ma, S. Zou, R. Li, X. Peng, S. Dai and J. Fan, *Chem. Commun.*, 2013, **49**, 7274–7276.

[7] M. Wuithschick, B. Paul, R. Bienert, A. Sarfraz, U. Vainio, M. Sztucki, R. Kraehnert, P. Strasser, K. Rademann, F. Emmerling and J. Polte, *Chem. Mater.*, 2013, **25**, 4679–4689.

[8] A. Villa, G.M. Veith and L. Prati, *Angew. Chem. Int. Ed.*, 2010, **49**, 4499−4502.

[9] S.E. Davis, M.S. Ide and R.J. Davis, *Green Chem.*, 2013, **15**, 17–45.

[10] A. Tanaka, K. Hashimoto and H. Kominami, *J. Am. Chem. Soc.*, 2012, **134**, 14526−14533.

[11] D.I. Enache, D.W. Knight and G.J. Hutchings, *Catal. Lett.*, 2005, **103**, 43–52.

[12] M. Boronat, A. Corma, F. Illas, J. Radilla, T. Ródenas and M.J. Sabater, *J. Catal.*, 2011, **278**, 50–58.

[13] A. Villa, C.E. Chan-Thaw, G.M. Veith, K.L. More, D. Ferri and L. Prati, *ChemCatChem*, 2011, **3**, 1612–1618.

[14] G.L. Hallett-Tapley, M.J. Silvero, C.J. Bueno-Alejo, M. González-Béjar, C.D. McTiernan, M. Grenier, J.C. Netto-Ferreira and J. C. Scaiano, *J. Phys. Chem. C*, 2013, **117**, 12279–12288.

[15] W. Fang, J. Chen, Q. Zhang, W. Deng and Y. Wang, *Chem. Eur. J.*, 2011, **17**, 1247–1256.

[16] C. Xu, J. Sun, B. Zhao and Q. Liu, *Appl. Catal. B*, 2010, **99**, 111–117.

[17] G.L. Brett, Q. He, C. Hammond, P.J. Miedziak, N. Dimitratos, M. Sankar, A.A. Herzing, M. Conte, J.A. Lopez-Sanchez, C.J. Kiely, D.W. Knight, S.H. Taylor and G.J. Hutching, *Angew. Chem. Int. Ed.*, 2011, **50**, 10136–10139.

[18] P. Liu, Y. Guan, R.A. van Santen, C. Li and E.J.M. Hensen, Chem. Commun. 2011, **47**, 11540–11542.

[19] C. Jia, Y. Liu, H. Bongard and F. Schüth, *J. Am. Chem. Soc.*, 2010, **132**, 1520–1522.

[20] M.A. Brown, Y. Fujimori, F. Ringleb, X. Shao, F. Stavale, N. Nilius, M. Sterrer and H. Freund, *J. Am. Chem. Soc.*, 2011, **133**, 10668–10676.

[21] J. Dupin, D. Gonbeau, P. Vinatier and A. Levasseur, *Phys. Chem. Chem. Phys.*, 2000, **2**, 1319–1324.

[22] A. Abad, P. Concepción, A. Corma and H. García, *Angew. Chem. Int. Ed.*, 2005, **44**, 4066–4069.

[23] M. Wang, J. Ma, C. Chen, F. Lu, Z. Du, J. Cai and J. Xu, *Chem. Commun.*, 2012, **48**, 10404–10406.

[24] B.K. Min and C.M. Friend, *Chem. Rev.*, 2007, **107**, 2709–2724.

[25] G. Zhao, J. Huang, Z. Jiang, S. Zhang, L. Chen and Y. Lu, *Appl. Catal. B*, 2013, **140–141**, 249–257.

Figure captions

Fig. 1 XRD patterns of catalysts before and after calcination (a) Au/γ-Al_2O_3, (b) Au/HT, (c) Au/HT calcined at 500 °C, (d) Au/MgO (e) Au/MgO calcined at 500 °C.

Fig. 2 TEM images of catalysts before and after calcination (a_1–a_3) Au/HT, (b_1–b_3) Au/MgO, (c_1–c_3) Au/γ-Al_2O_3 (1: SI, 2: DP, 3: IMP; -cn: calcined at 500 °C).

Fig. 3 STEM images and gold size distribution of Au/HT by IMP method (a) before calcination and (b) after calcination.

Fig. 4 The XPS spectra of O 1s for Au/MgO by IMP method (a) before calcination and (b) after calcination.

Fig. 5 The XPS spectra of Mg 2s and Au 4f for Au/MgO by IMP method (a) before calcination and (b) after calcination.

Table captions

Table 1 BET Surface area and pore diameter distribution of supports

Table 2 Catalytic performance of catalysts before and after calcination

Table 3 Basic strength and basicity of supports

Table 4 Recycling experiments of catalysts[a]

Table 1 BET Surface area and pore diameter distribution of supports

Entry	Supports	Surface area[a] ($m^2\ g^{-1}$)	Pore volume[b] ($cm^3\ g^{-1}$)	Pore diameter[b] (Å)
1	$Mg(OH)_2$	19	0.21	434
2	MgO	174	0.46	105
3	Rehydrated $Mg(OH)_2$	53	0.39	296
4	HT	16	0.08	212
5	Mg(Al)O	145	0.29	78
6	γ-Al_2O_3	188	0.56	119

[a] Calculated by the BET method. [b] Calculated by the BJH method from the desorption isotherm.

Table 2 Catalytic performance of catalysts before and after calcination

Entry	Catalyst	Preparation method	Gold particles (nm)		Conversion of benzyl alcohol (%)		Benzaldehyde yield (%)		Selectivity to benzaldehyde (%)		TOF (h^{-1})[c]	
			Before[a]	After[b]	Before[a]	After[b]	Before[a]	After[b]	Before[a]	After[b]	Before[a]	After[b]
1	Au/HT	SI	3.0	-[d]	100	39	98	19	98	49	670	240
2	Au/MgO	SI	3.4	-[d]	95	87	91	71	96	82	494	225
3	Au/γ-Al_2O_3	SI	3.5	-[d]	99	73	79	51	79	70	552	405
4	Au/HT	DP	8.1	11.9	98	100	69	76	70	76	459	493
5	Au/MgO	DP	8.4	12.1	51	100	43	81	84	81	230	314
6	Au/γ-Al_2O_3	DP	3.4	6.5	98	99	67	74	68	75	489	478
7	Au/HT	IMP	6.4	11.4	83	98	69	97	83	99	280	356
8	Au/MgO	IMP	5.2	46	87	100	65	87	75	87	295	371
9	Au/γ-Al_2O_3	IMP	3.0	5.0	96	99	81	86	84	87	441	458

[a] Catalyst before calcination, [b] Catalyst after calcination, [c] TOF calculated after 30 min reaction for 0.05 g catalyst. [d] Part of gold particles coagulated.

Table 3 Basic strength and basicity of supports

Entry	Supports	Basic strength	Basicity at H_-=7.2–9.3 (mmol/g)	Basicity at H_->9.3 (mmol/g)	Total basicity (mmol/g)
1	HT	9.3< H_-<11	0.15	0.15	0.30
2	Mg(Al)O	12.2< H_-<15	0.23	0.34	0.57
3	$Mg(OH)_2$	9.3< H_-<11	0.21	0.15	0.36
4	MgO	12.2< H_-<15	0.53	0.45	0.98
5	Rehydrated $Mg(OH)_2$	9.3< H_-<11	0.23	0.19	0.42
6	γ-Al_2O_3	7.2< H_-<9.3	0.08	0.03	0.11

Table 4 Recycling experiments of catalysts[a]

Catalysts	The difference between size of gold particles before reaction and after second run (nm)	Number of catalyst uses	Conversion of benzyl alcohol (%)	Benzaldehyde yield (%)	Selectivity to benzaldehyde (%)
Au/HT	0.1	1st	100	98	98
		2nd	97	94	97
		3rd	85	79	93
		4th	73	68	93
Au/γ-Al_2O_3	0.5	1st	97	79	79
		2nd	57	35	61
		3rd	38	16	42
Au/MgO	Part of gold particles coagulated	1st	95	91	96
		2nd	31	30	97

[a] The spent catalyst was washed with toluene for three times, dried at 100 °C in air, and then applied to the further run without any other treatment.

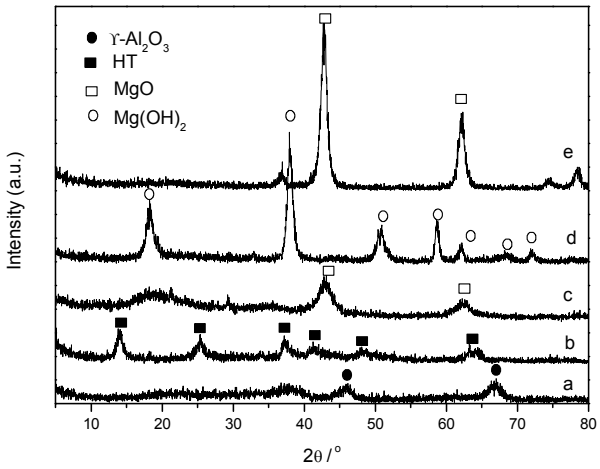

Fig. 1 XRD patterns of catalysts before and after calcination (a) Au/γ-Al_2O_3, (b) Au/HT, (c) Au/HT calcined at 500 °C, (d) Au/MgO, (e) Au/MgO calcined at 500 °C.

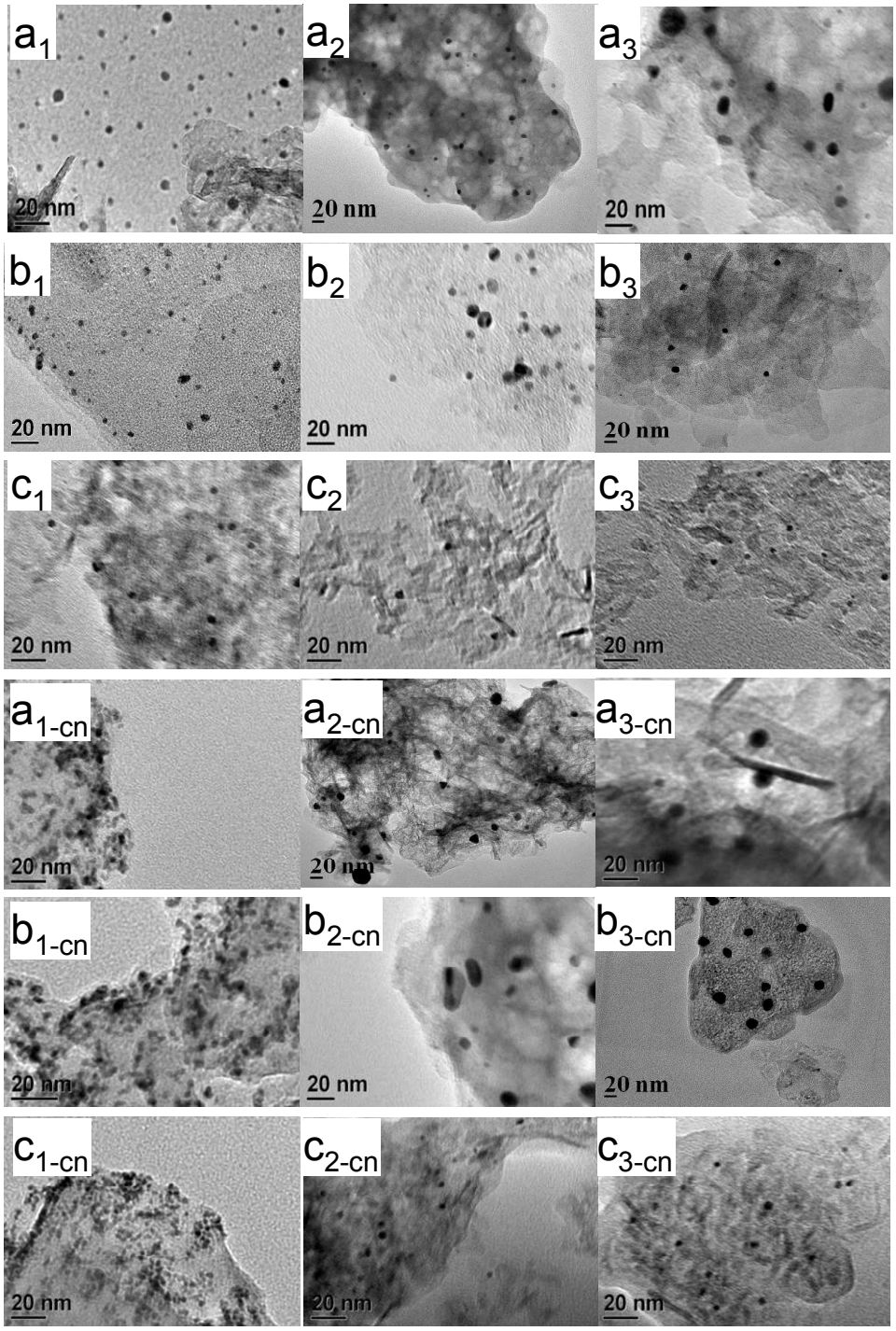

Fig. 2 TEM images of catalysts before and after calcination (a_1–a_3) Au/HT, (b_1–b_3) Au/MgO, (c_1–c_3) Au/γ-Al_2O_3 (1: SI, 2: DP, 3: IMP; -cn: calcinated at 500 °C).

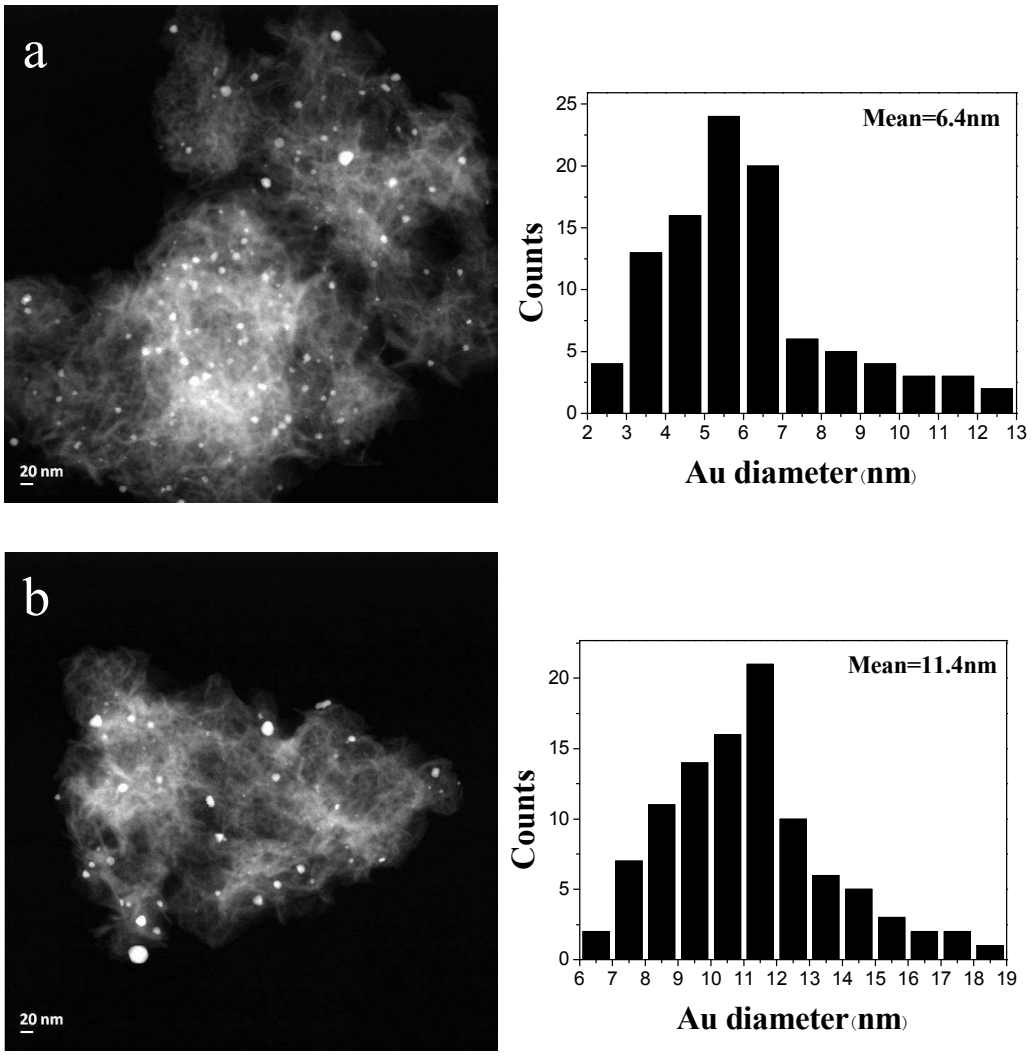

Fig. 3 STEM images and gold size distribution of Au/HT by IMP method (a) before calcination and (b) after calcination.

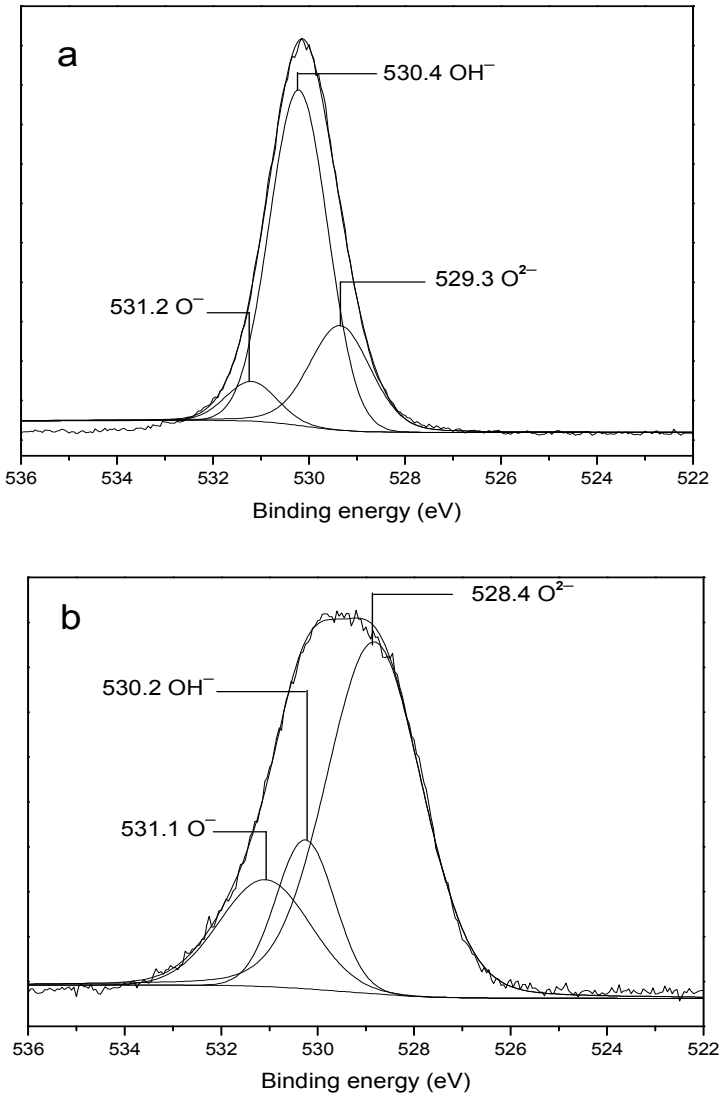

Fig. 4 The XPS spectra of O 1s for Au/MgO by IMP method (a) before calcination and (b) after calcination.

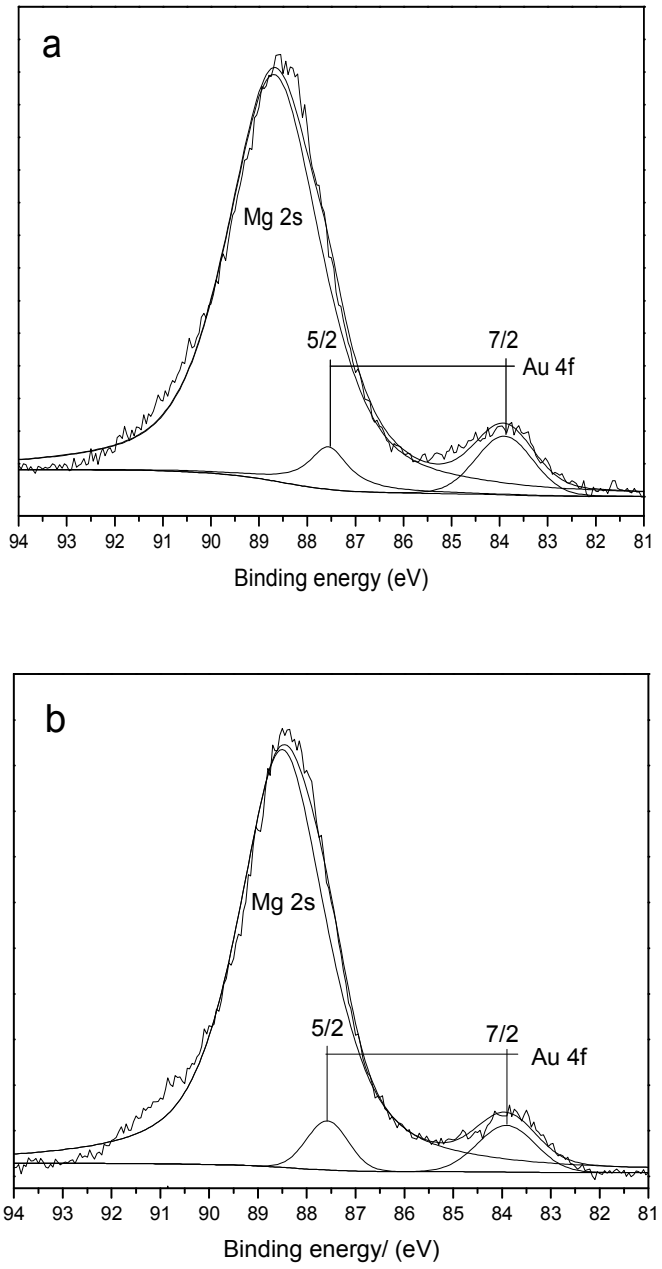

Fig. 5 The XPS spectra of Mg 2s and Au 4f for Au/MgO by IMP method (a) before calcination and (b) after calcination.

Graphical abstract